Electronic Supplementary Material (ESI) for Reaction Chemistry & Engineering.

Electronic Supplementary Information for

A new systematic synthesis of ultimate nickel nanocatalysts for compact hydrogen generation

Hack-Keun Lee,[†a] *Shin Wook Kang,*[†a] *Jung-Il Yang,*[a] *Dong Hyun Chun,*[b] *Jin Hee Lee,*[a]
Dawon Oh,[a] *Jungmin Ban,*[a] *Taesung Jung,*[b] *Heon Jung,*[a] *Ji Chan Park*[*,a]

[a] Clean Fuel Research Laboratory, Korea Institute of Energy Research, Daejeon 34129, Korea

[b] Carbon Conversion Research Laboratory, Korea Institute of Energy Research, Daejeon 34129, Korea

E-mail: jcpark@kier.re.kr

† H. K. Lee and S. W. Kang contributed equally to this work

Experimental Section

Chemicals: Nickel (II) nitrate hexahydrate ($Ni(NO_3)_2 \cdot 6H_2O$, ≥98 %, DAEJUNG), gamma-alumina powder (γ–Al_2O_3, Alfa Aesar), Santa Barbara Amorphous-15 (SBA-15, SiO_2, ACS Material), activated charcoal (Aldrich), and silica-alumina (SiO_2-Al_2O_3, Aldrich) were used as received without further purification. The commercial FCR catalyst (Sud-Chemie) was used as a control for comparing the performance of the prepared catalysts.

Synthesis of ultimate Ni nanocatalysts: For synthesis of the u-Ni/Al_2O_3 nanocatalyst, a mixed powder (0.8 g) in a ratio of 1.65 $Ni(NO_3)_2 \cdot 6H_2O$ to alumina support (0.3 g) was prepared using a high-energy ball mill (SPEX 8000M Mixer/Mill®). The SUS reactor (18 mm outer diameter, 1.0 mm wall thickness, 115 mm height) containing the powdered mixture, was placed in a sample holder of the AIO reaction apparatus. Then, the automated sequence consisting of aging, heating, and calcination proceeded within the set values (Table 1). After the sequence, the resulting black powder was cooled to room temperature, and then was submerged in ethanol (20 mL) to prevent rapid surface oxidation of the active Ni particles. Finally, the u-Ni/Al_2O_3 nanocatalyst immersed in ethanol was separated using a magnet and dried in a vacuum oven at 323 K. For the preparation of u-Ni/AC nanocatalyst and u-Ni/SiO_2-Al_2O_3 nanocatalyst, all procedures and conditions were identical to that for the u-Ni/Al_2O_3 nanocatalyst except the use of activated charcoal and silica-alumina powder as the catalyst support.

Steam-methane-reforming experiments: Catalytic reaction tests were performed in a fixed bed continuous flow reactor operated at atmospheric pressure. A portion (0.1 g) of the catalysts was placed in the center of a tube-type quartz reactor (1/4 inch outer diameter, 1.0 mm wall thickness). The reactor temperature was slowly increased to 973 K with a ramping rate of 15 $K \cdot min^{-1}$ under hydrogen gas. After pre-treatment at 700 °C for 1 h under a hydrogen flow (100 $mL \cdot min^{-1}$), a mixture of methane (25 vol%) and steam (75 vol%) was introduced at 700 °C with a space velocity of 50, 100, and 200 $NL \cdot h^{-1} \cdot g_{cat}^{-1}$. The reaction products were analyzed using gas chromatography (iGC7200, DS Science Inc.), and catalyst activities were measured by conducting a time-on-stream study at 700 °C for 4 h. The CH_4 conversion (X_{CH4}) was calculated from the following equation.

$$CH_4 \text{ conv. } (\%) = ([CH_4]_{in} - [CH_4]_{out})/([CH]_{in}) \times 100$$

Characterization: Transmission electron microscopy (TEM) images were obtained using a Talos F200X operated at 200 kV. Energy-disperse X-ray spectroscopy (EDS) elemental mapping was performed using a higher-efficiency detection system (Super X: 4 windowless SDD EDS system). The X-ray diffraction (XRD) patterns of the samples were recorded on a high-power powder X-ray diffractometer (Rigaku D/MAX-2500, 18 kW). The N_2 sorption isotherms were measured at 77 K with a TriStar II 3020 surface area analyzer. Before measurement, the samples were degassed in a vacuum at 573 K for 4 h. CO chemisorption measurements were performed using a Micromeritics ASAP 2000C. Before measurement, the sample was dried and degassed at 200 °C for 4 h.

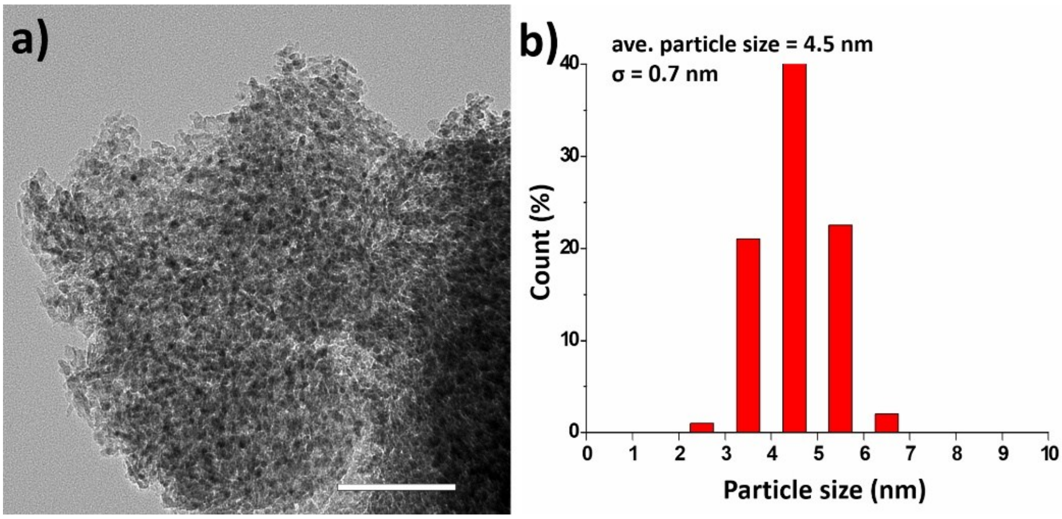

Figure S1. (a) Low-resolution TEM image and (b) Size distribution histograms of u-Ni/Al_2O_3 nanocatalyst. The bar represents 100 nm. The average Ni particle size was obtained from measurement of 200 particles in the TEM images.

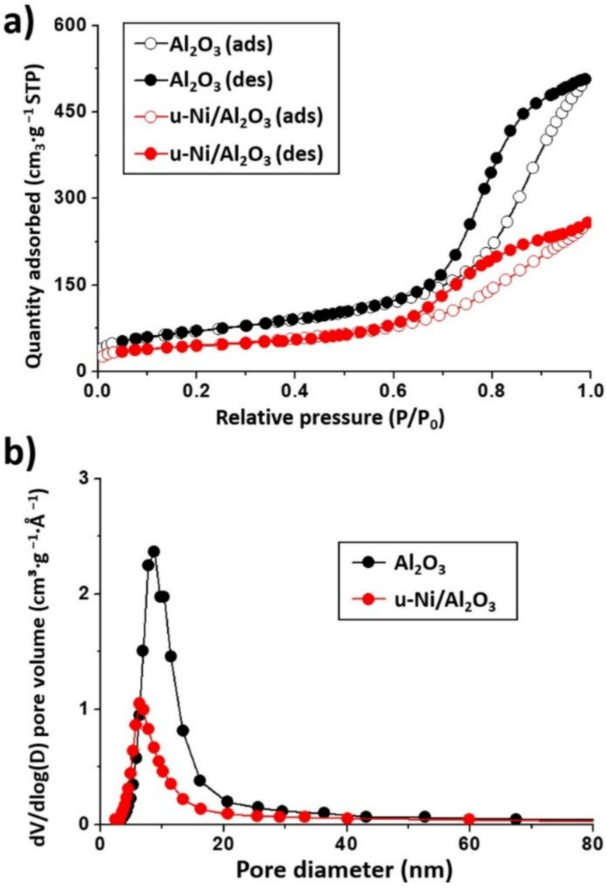

Figure S2. (a) N_2 adsorption/desorption isotherms and (b) Pore size distribution diagrams of pristine graphene and u-Ni/Al_2O_3 nanocatalyst calculated from desorption branches using the BJH method.

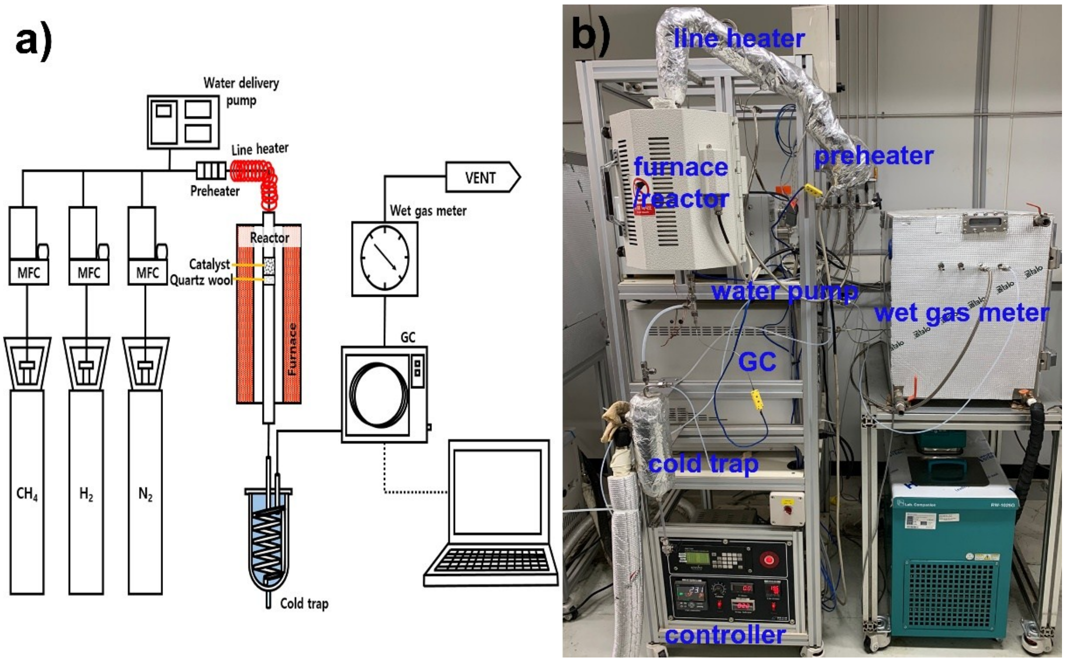

Figure S3. (a) Schematic diagram and (b) Photograph of the SMR reaction system.

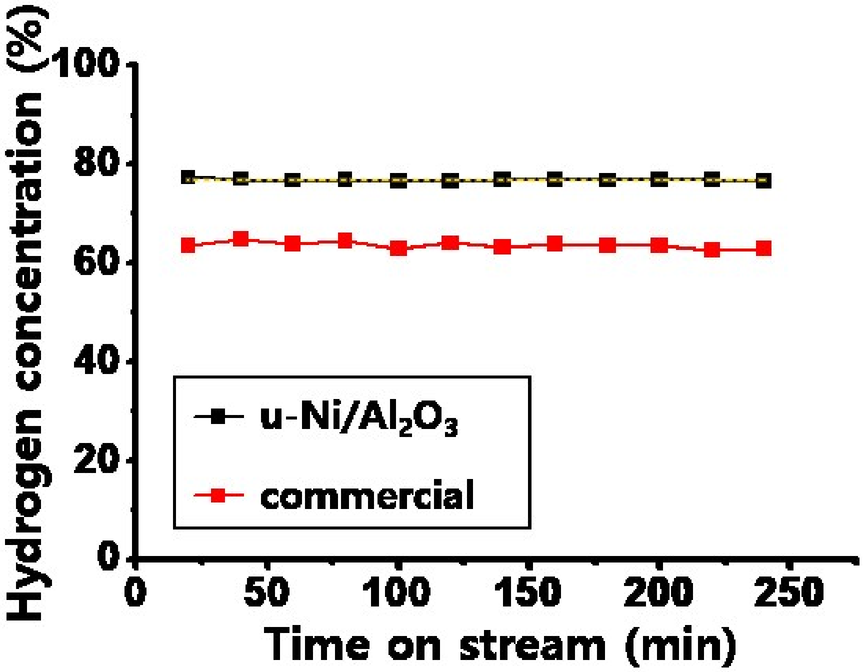

Figure S4. Hydrogen concentration graphs by u-Ni/Al$_2$O$_3$ nanocatalyst and commercial Ni catalyst. The reactions were performed at 973 K with H_2O/CH_4 ratio = 3 and GHSV = 100 $NL{\cdot}g_{cat}^{-1}{\cdot}h^{-1}$. The dotted yellow line indicates hydrogen concentration at thermodynamic equilibrium.

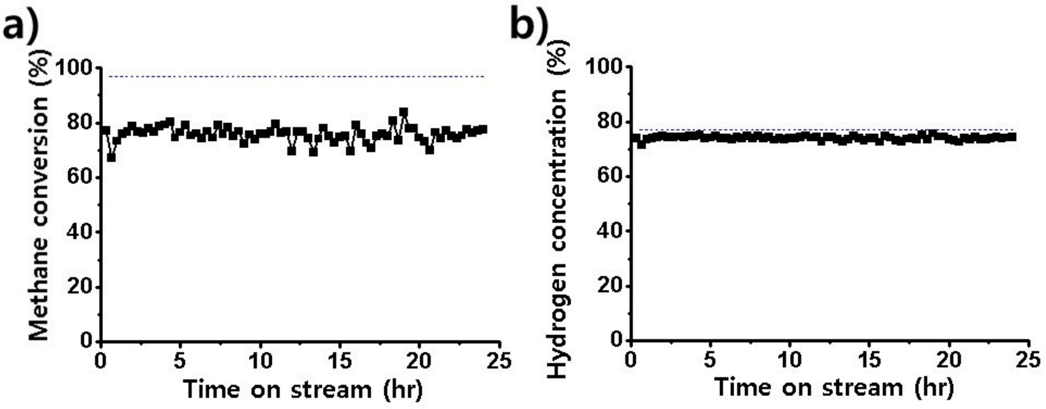

Figure S5. Long-term catalyst performance profile for SMR reaction on u-Ni(25wt%)/Al_2O_3 nanocatalyst at GHSV = 200 NL·g_{cat}^{-1}·h^{-1} for 24 h. (a) Methane conversion and (b) hydrogen concentration. The reaction was performed under H_2O:CH_4 = 3:1. Dotted blue lines indicate methane conversion and hydrogen concentration at thermodynamic equilibrium, respectively.

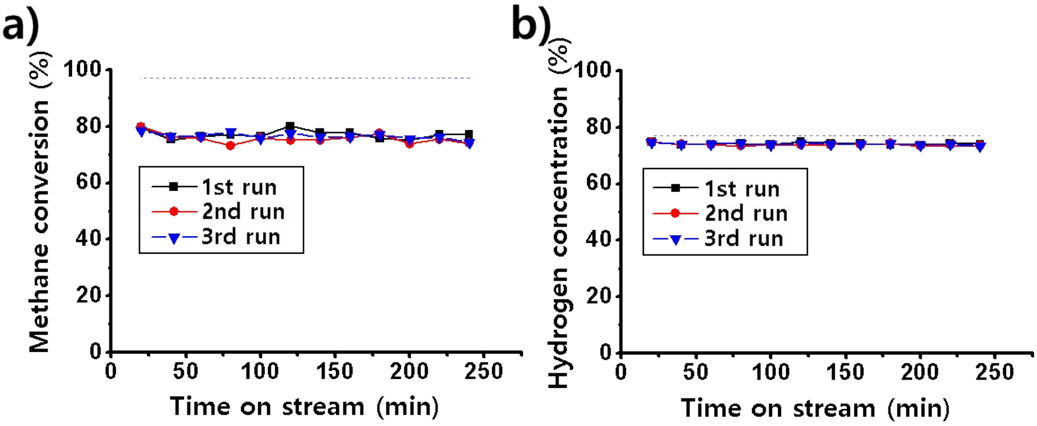

Figure S6. Recycling tests for SMR reaction on u-Ni(25wt%)/Al_2O_3 nanocatalyst at GHSV = 200 NL·g_{cat}^{-1}·h^{-1}. (a) Methane conversion and (b) hydrogen concentration. The reaction was performed under H_2O:CH_4 = 3:1. Dotted blue lines indicate methane conversion and hydrogen concentration at thermodynamic equilibrium, respectively.

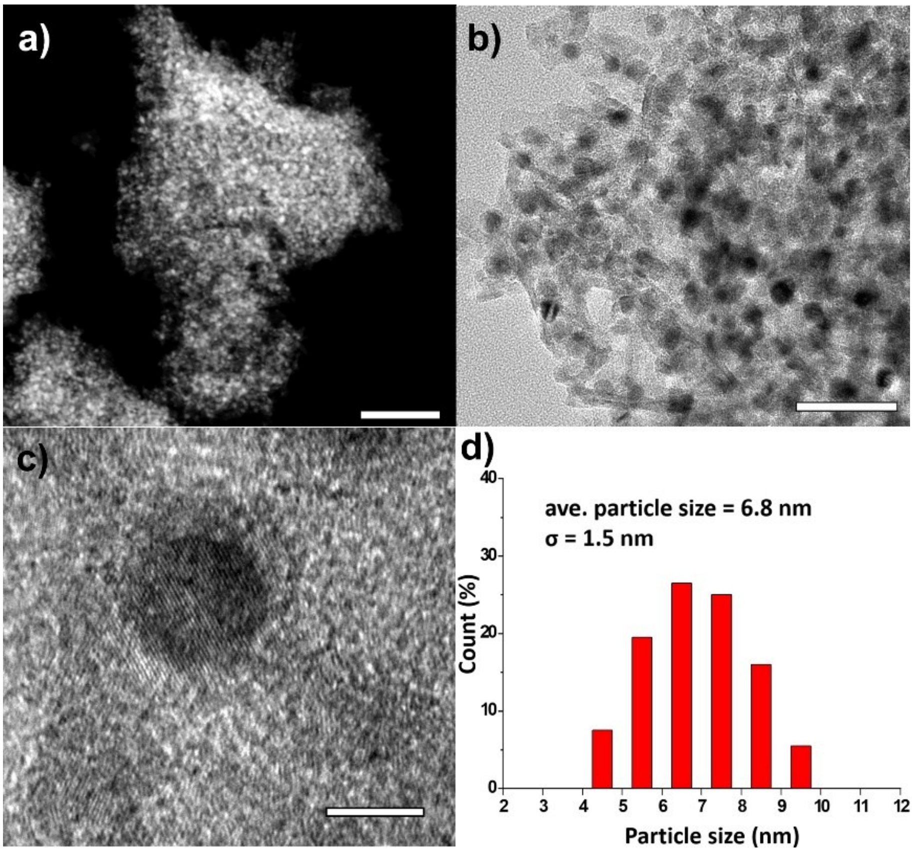

Figure S7. (a) Low-resolution HAADF-TEM, (b) magnified TEM, (c) HR-TEM image, and (d) size distribution histogram of the recovered u-Ni/Al_2O_3 nanocatalyst from the SMR reaction at 973 K. The bars represent 200 nm (a), 50 nm (b), and 5 nm (c).

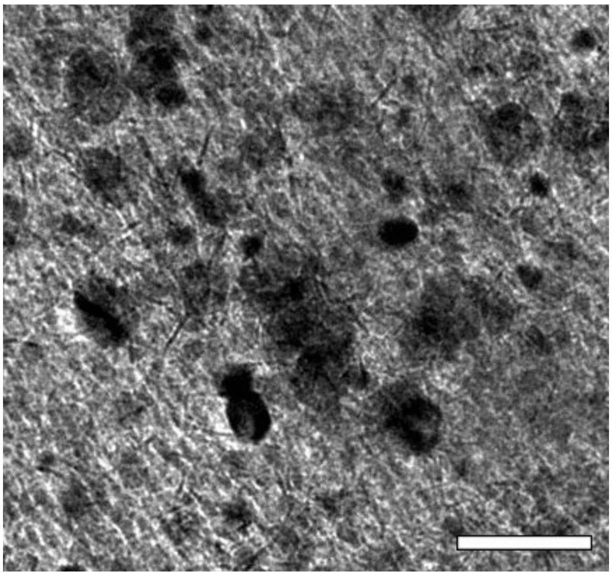

Figure S8. TEM image of the recovered Ni/SBA-15 nanocatalyst from the SMR reaction at 973 K. The bar represents 50 nm.

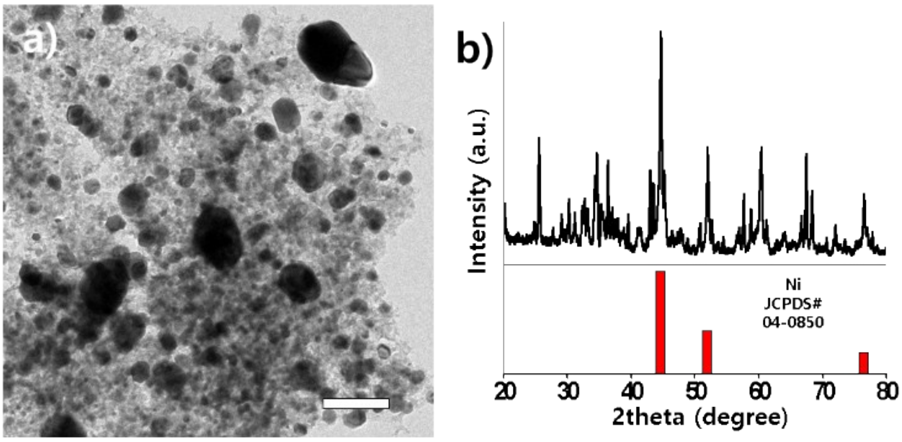

Figure S9. (a) TEM image and (b) XRD spectrum of commercial FCR catalyst recovered after the SMR reaction at 973 K. The bar represent 200 nm.

Table S1. Comparison data of Ni-based catalysts in SMR reactions.

Catalyst	Ni (wt%)	Particle size (nm)	Rxn. temp. (°C)	GHSV ($NL \cdot g_{cat}^{-1} \cdot h^{-1}$)	H_2O/CH_4	CH_4 conv. (%)	H_2 conc. (%)	H_2 productivity ($mol_{H2} \cdot g_{cat}^{-1} \cdot h^{-1}$)	ref.
u-Ni/Al_2O_3	25	4.3	700	50	3	96.7	~77	1.87	This work
				100		91.8	76.5	3.57	
				200		78.0	73.9	6.06	
Ni/SBA-15		24.0		100		67.0	70.4	2.64	
Commercial Ni cat.	-	-		50		83.1	75.6	1.68	
				100		62.5	69.6	2.57	
				200		40.2	59.5	3.25	
Ni/Ce–ZrO_2/θ-Al_2O_3	12	-		10		97	~77	~0.34[a]	[1]
Ni/SiO_2 yolk-shell diluted with SiO_2	20	24		25		85	70	~0.78[a]	[2]
NiO-SiO_2/Al_2O_3	8.8	10.7		8.9	3.5	95.7	~73	0.29[a]	[3]
Ni/gadolinia-doped ceria	5	24.5		1.9	2	65.2		0.06	[4]
Ni/$Y_2Ti_2O_7$		9.1		36		82		1.27	[5]
Ni/γ-Al_2O_3	20	-	738	8.8	3	97.9	75	0.32	[6]
Ni/$MgAl_2O_4$			750	54	2	97.2	71.5		[7]

a) We assumed that the flow rates of outlet gases are about 4 times the reactant CH_4 flow rate in the SMR reactions.

References)

[1] Y.-S. Oh, H.-S. Roh, K.-W. Jun, Y.-S. Baek, *Int. J. Hydrog. Energy* **2003**, 28, 1387.

[2] J. C. Park, J. U. Bang, J. Lee, C. H. Ko, H. Song, *J. Mater. Chem*. **2010**, 20, 1239.

[3] B. Bej. N. C. Pardhan, S. Neogi, *Catal. Today* **2013**, 207, 28.

[4] T.-J. Huang, M.-C. Huang, *Chem. Eng. J.* **2008**, 149, 153.

[5] L. Xia, X. Fang, X. Xu, Q. Liu, M. Yang, J. Xu, Z. Gao, X. Wang, *Int. J. Hydrog. Energy* **2020**, 45, 14556.

[6] J.-I. Yang, T. W. Kim, J. C. Park, T.-H. Lim, H. Jung, D. H. Chun, *Int. J. Hydrog. Energy* **2016**, 41, 8176.

[7] H.-W. Kim, K.-M. Kang, H.-Y. Kwak, J. H. Kim, *Chem. Eng. J*. **2011**, 168, 775.